The route to fullerenoid oxides

MARYVONNE HERVIEU*, BENJAMIN MELLÈNE, RICHARD RETOUX, SOPHIE BOUDIN AND BERNARD RAVEAU

Laboratoire CRISMAT, UMR 6508 CNRS ENSICAEN, 6 bd Maréchal Juin, 14050 CAEN Cedex 4, France
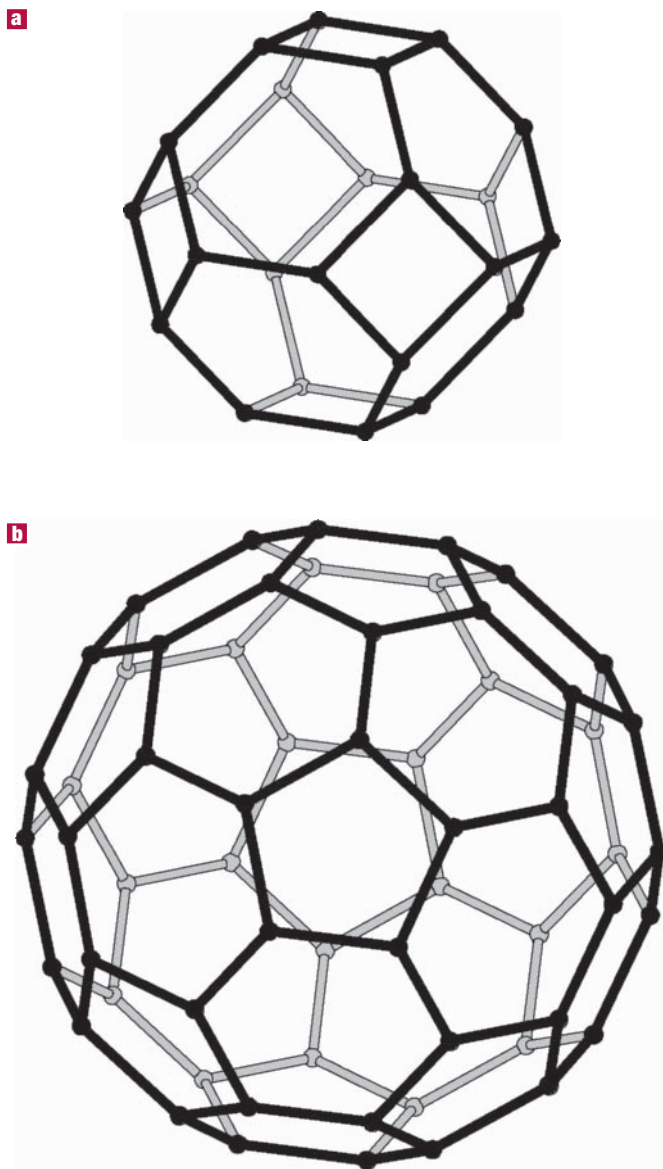*e-mail: maryvonne.hervieu@ismra.fr

Tetrahedral oxides, like silicates and aluminates, have attracted great interest due to their potential for numerous applications in various fields ranging from catalysis, ion exchange and molecular sieves, to thermo- and photoluminescence. In spite of their tetrahedral character, no effort has been made to date for establishing structural relationships between these tetrahedral oxides with different forms of carbon, for example, fullerenes. Here, we report for the first time an oxide that exhibits a three-dimensional framework of AlO_4 tetrahedra forming huge 'Al$_{84}$' spheres, similar to those of the $D2d$ isomer of the C_{84} fullerenes. These Al$_{84}$ spheres, displayed in a face-centred-cubic lattice, are easily identified by high-resolution electron microscopy. We also show that this $Sr_{33}Bi_{24+\delta}Al_{48}O_{141+3\delta/2}$ aluminate exhibits an onion-skin-like subnanostructure of its Bi/Sr/O species located inside the Al$_{84}$ spheres. The role of the original pseudo-spheric anion $[Bi_{16}O_{52-n}\square_n]$—with n vacancies ($\square$)—in the stabilization of such a structure is discussed. This structure seems to be promising for the generation of a large family of fullerene-type (fullerenoid) oxides with various properties.

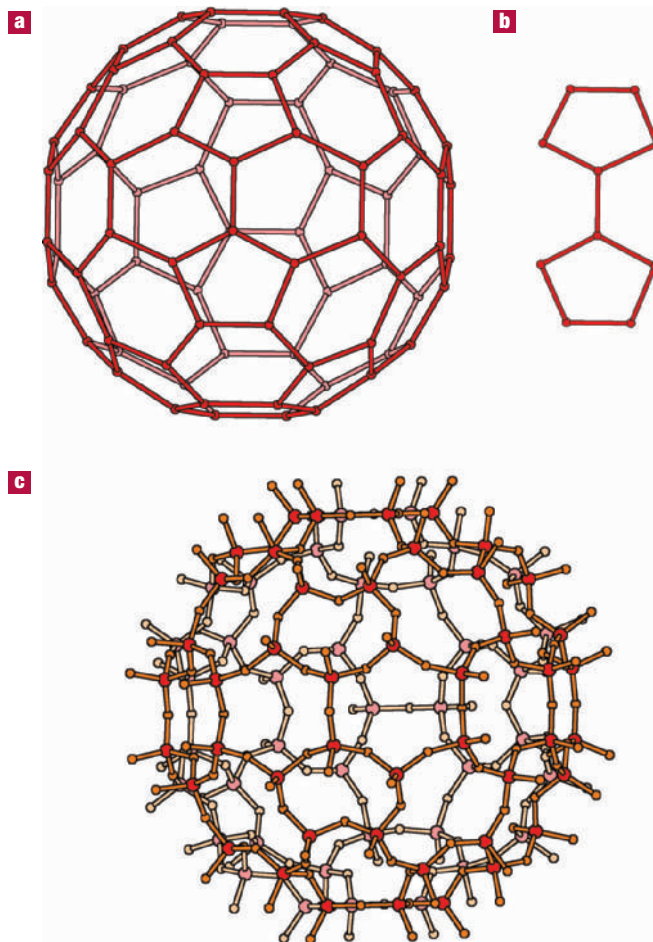Tetrahedral oxides involving species such as Si and Al have received considerable attention due to their great potential for various applications. Several strontium aluminates have indeed been recently studied as pigments for photoluminescence or thermoluminescence[1], whereas silicates and silicoaluminates of the zeolite and ultramarine family are currently investigated for their adsorptive and ion-exchange properties, their behaviour as molecular sieves and their catalytic properties[2–8]. These oxides exhibit various complex structures, which can be better understood by considering their topology[9,10], so that each tetrahedron is currently represented by its metallic (M) atom (Al or Si), allowing the large cavities and tunnels to be easily identified in the three-dimensional (3D) frameworks, by connecting Al or Si atoms by straight lines (see refs 11,12 for a review). Bearing in mind this mode of representation, it is of interest to compare the M = Si, Al frameworks of zeolites with those of fullerenes. This is illustrated, for instance, for the sodalite cage of ultramarine $Na_{8–10}Al_6Si_6O_{24}S_{2–4}$ (Fig. 1a) built up of hexagonal (Al, Si)$_6$ and square (Al, Si)$_4$ 'windows'. This sodalite cage can be compared to the C_{60} fullerene[13] (Fig. 1b), which consists of C_{60} spheric molecules built up of edge-sharing C_5 pentagons and C_6 hexagons. This topologic analysis suggests that it should be possible to synthesize fullerenoid oxides in which metallic atoms would form, similarly to fullerenes—bucky balls—whose cohesion should be ensured by oxygen atoms located half the distance between two metallic atoms, so that each metallic atom would exhibit a tetrahedral coordination. In this paper, we report the first fullerenoid oxide, which consists of Al$_{84}$ spheres similar to one of the fullerene C_{84} isomers[14], and we show that the Al$_{84}$ spheres form a face-centred-cubic array 3D framework.

Our strategy for the synthesis of fullerenoid oxides is based on the fact that the realization of such M$_n$ spheres in the form of a 3D framework of tetrahedra requires the M$_n$ spheres to be stuffed with voluminous species to ensure the stability of the structure. Each $M_nO_{(3n+2)/2}$ sphere could be stabilized by various organic templates (ions or molecules), using hydrothermal synthesis, but it is a risk to introduce hydroxyl groups in the framework, as this is likely to decrease the stability of the materials. The second possibility is to introduce large

Figure 2 Al_{84} and C_{84} fullerene. a,b, The Al_{84} spheres (**a**) are similar to the D_2d isomer of the C_{84} fullerene, and exhibit pentagon pairs (**b**). **c**, The tetragonal coordination of the Al generates $Al_{84}O_{120}$ spheres.

Figure 1 Ultramarines and C_{60} fullerene. a,b, The geometry of the sodalite cage of ultramarines (**a**) can be considered as a quasi dual form of the spheric molecules of C_{60} fullerene (**b**).

cations to neutralize the negative charges formed by the $M_nO_{(3n+2)/2}$ spheres. We have prioritized this second direction of research, as it should allow the procedure to be done under normal pressure. Consideration of the previous studies carried out on 3D aluminates shows that among the numerous compounds that have been isolated, the aluminate $Sr_6Bi_2O_3(AlO_2)_{12}$ (ref. 15) is of great interest, as its tetrahedral framework $[AlO_2]_\infty$ forms large cavities and tunnels where Sr^{2+} cations and Bi_2O_3 groups are located. Starting from this observation, we have revisited the system $SrO–Bi_2O_3–Al_2O_3$. During this investigation we have isolated the aluminate $Sr_{33}Bi_{24+\delta}Al_{48}O_{141+3\delta/2}$ by solid-state reaction, starting from a mixture of SrO, Bi_2O_3 and Al_2O_3. Single crystals of this new aluminate were also grown and studied by X-ray diffraction. The detailed method for synthesis, crystal growth and structure determination will be reported elsewhere.

This aluminate exhibits a large cubic cell, $a = 25.09$ Å, and belongs to the space group $F\bar{4}3m$, containing four formulae per unit cell. Its crystal structure appears, at first sight, rather complex: it has a 3D framework of corner-sharing AlO_4 tetrahedra, forming large spherical cages containing Sr^{2+} cations and bismuth–oxygen clusters. Moreover, additional Sr^{2+} cations sit between the cages.

The first important feature of this structure deals with the aluminium lattice. The aluminium atoms form huge spheres Al_{84} (Fig. 2a), built up of Al_5 pentagons and Al_6 hexagons, similarly to the fullerenes. In fact, this configuration characterized by pentagon pairs (Fig. 2b) corresponds to the $D2d$ isomer, the one most currently encountered for the C_{84} fullerene[14]. Nevertheless, the size of the Al_{84} sphere is much larger than that of the C_{84} fullerene, showing a diameter of 18.5 Å, compared with 8.5 Å for C_{84}. This great size difference is due to the oxygen atoms, located approximately half way between two adjacent aluminium atoms, so that the Al_{84} sphere generates an $Al_{84}O_{210}$ sphere of corner-sharing AlO_4 tetrahedra (Fig. 2c).

The second remarkable characteristic concerns the arrangement of the Al_{84} spheres, which form a face-centred-cubic array as shown from the projection of the aluminium lattice along the [100] direction (Fig. 3). Moreover, each Al_{84} sphere shares a hexagonal Al_6 face with twelve other identical spheres forming the $[Al]_\infty$ 3D framework. In this
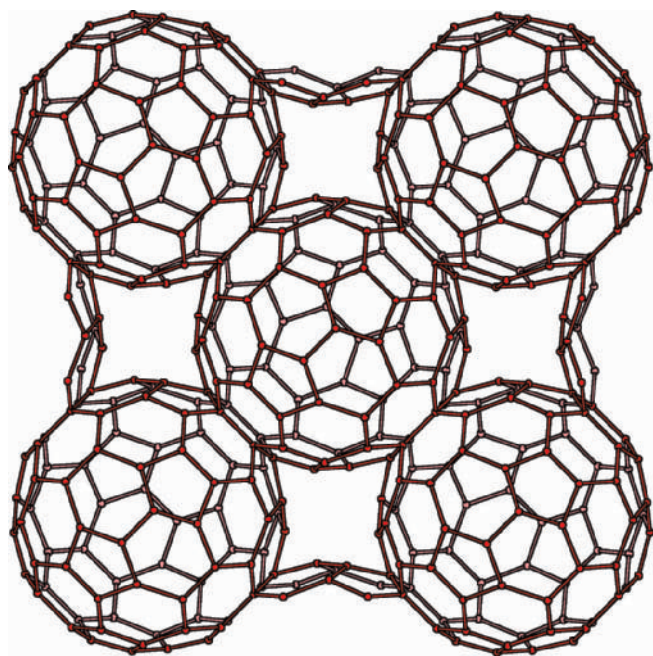
Figure 3 Projection of the Al framework of the bismuth aluminate $Sr_{33}Bi_{24+\delta}Al_{48}O_{141+3\delta/2}$ along [100], showing a face-centred-cubic array of spheres sharing Al_6 hexagons.

Figure 4 The onion-skin-like subnanostructure of the BiSrO array contained in the Al_{84} spheres of $Sr_{33}Bi_{24+\delta}Al_{48}O_{141+3\delta/2}$. The colours refer to those adopted in Fig. 5.

respect, the aluminium network in this aluminate is very different from the fullerenes, in which the C_n spheres are isolated. Regarding the oxygen network, it is worth pointing out that one oxygen atom per aluminium atom is located outside of the Al_{84} sphere. This means that 84 oxygen atoms per $Al_{84}O_{210}$ sphere are located outside of the sphere. Twelve of these oxygen atoms form Al–O–Al bridges between two spheres, leading to the 3D framework of AlO_4 tetrahedra. The other 72 oxygen atoms participate in the next Al_{84} spheres. The remaining 126 oxygen atoms (3/2 oxygen atoms per aluminium) plaster the wall inside the Al_{84} sphere, forming an O_{126} sphere.

The third exceptional structural property resides in the onion-skin-like subnanostructure of the 'BiSrO' array located inside the Al_{84} sphere as schematized in Fig. 4. The O_{126} sphere (Fig. 5a) is built up of corner-sharing triangular groups O_3 forming hexagonal O_6 and pentagonal O_5 windows similar to the Al_{84} spheres, but sharing corners instead of edges. Inside the O_{126} sphere, the strontium and a part of the bismuth sites form a third concentric sphere $Sr_{32}(Bi_{8.25}\square_{3.75})$ (Fig. 5b), which consists of two interpenetrated spheres, the Sr_{32} sphere (blue coloured) built up of edge-sharing four-sided Sr_4 and six-sided Sr_6 rings, and the partially occupied $Bi_{8.25}\square_{3.75}$ sphere (yellow coloured), built up of Bi_4 squares and Bi_3 triangles. The fourth O_{40} sphere (Fig. 5c) consists of O_3 triangles and O_4 squares. The fifth sphere is represented by the central group Bi_{16} (Fig. 5d), forming edge-sharing Bi_3 triangles with Bi–Bi distances ranging from 3.54 Å to 4.21 Å. Finally, inside the latter sphere there exists a truncated O_{12} tetrahedron (Fig. 5e), which is only 61.5% occupied.

These fascinating structural specificities are clearly illustrated by the high-resolution electron microscopy (HREM) images. Two examples are given in Fig. 6. In the first image (Fig. 6a), recorded for a focus value close to Scherzer (close to –300 Å for the microscope), the high-electron-density zones appear as darker spots. The contrast of this
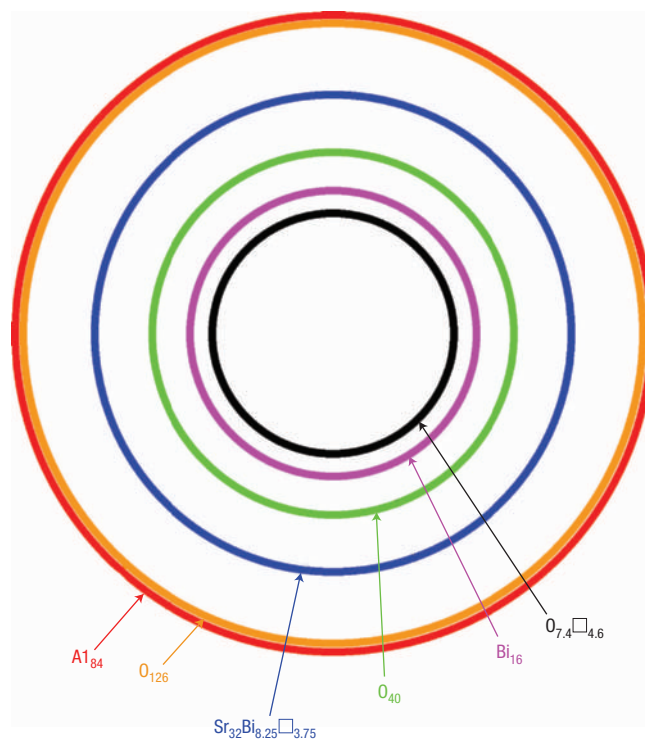
image can be described through a regular arrangement of dark butterfly wings, surrounded by darker crowns and separated by white crosses along [110] and single white dots elongated along [100] and [010]. The origin of the contrast is explained in Fig. 6b through the [001] projection of a single unit cell and an enlarged image. Two of the darker crowns surrounding the butterfly wings are represented by circles; and are drawn and superimposed on the image. The dark crown is associated to the complex projection of the atoms at the ball periphery and the butterfly wings to the positions of Bi and Sr atoms at the top of the spheres (see the projected structure). The white crosses of this Scherzer image are associated to the low electron density observed in between two tangent spheres in a compact plane and the elongated spots between two spheres located at different levels along c. The contrast generated by the $Sr_{32}(Bi_{8.25}\square_{4.75})$ spheres (observed for a focus value close to 50 Å) is most spectacular (Fig. 6c). It consists of an array of alternating white crosses and small white circles along [100] and [010]. Only the $Sr_{32}(Bi_{8.25}\square_{4.75})$ spheres are projected along [001] on the drawing in Fig. 6d. The white crosses are associated with the Sr and Bi atoms located at the top of the spheres and at the tangency area between two adjacent spheres located at the same level, whereas the small white circles are associated to projection of the Bi/Sr atoms located between spheres at different levels.

Attention must be drawn to the $Bi_{16}O_{52-n}\square_n$ anion, whose geometry is exceptional and is observed for the first time. This 'pseudo-spherical' anion (Fig. 7a) consists of six bipyramidal units Bi_2O_8 and four BiO_6 octahedra sharing their apices. In such an anion, the bipyramidal units are built up of two edge-sharing BiO_5 pyramids (Fig. 7b) whose apical apex is shared by three Bi_2O_8 units. The 12 oxygen atoms of the common edges are 61% occupied and form the truncated O_{12} tetrahedron. They also form three corners of each BiO_6 octahedron. The remaining oxygen atoms of the BiO_5 and BiO_6 polyhedra form the O_{40} sphere of the onion-skin-like structure. There is no doubt that the stereo-activity of
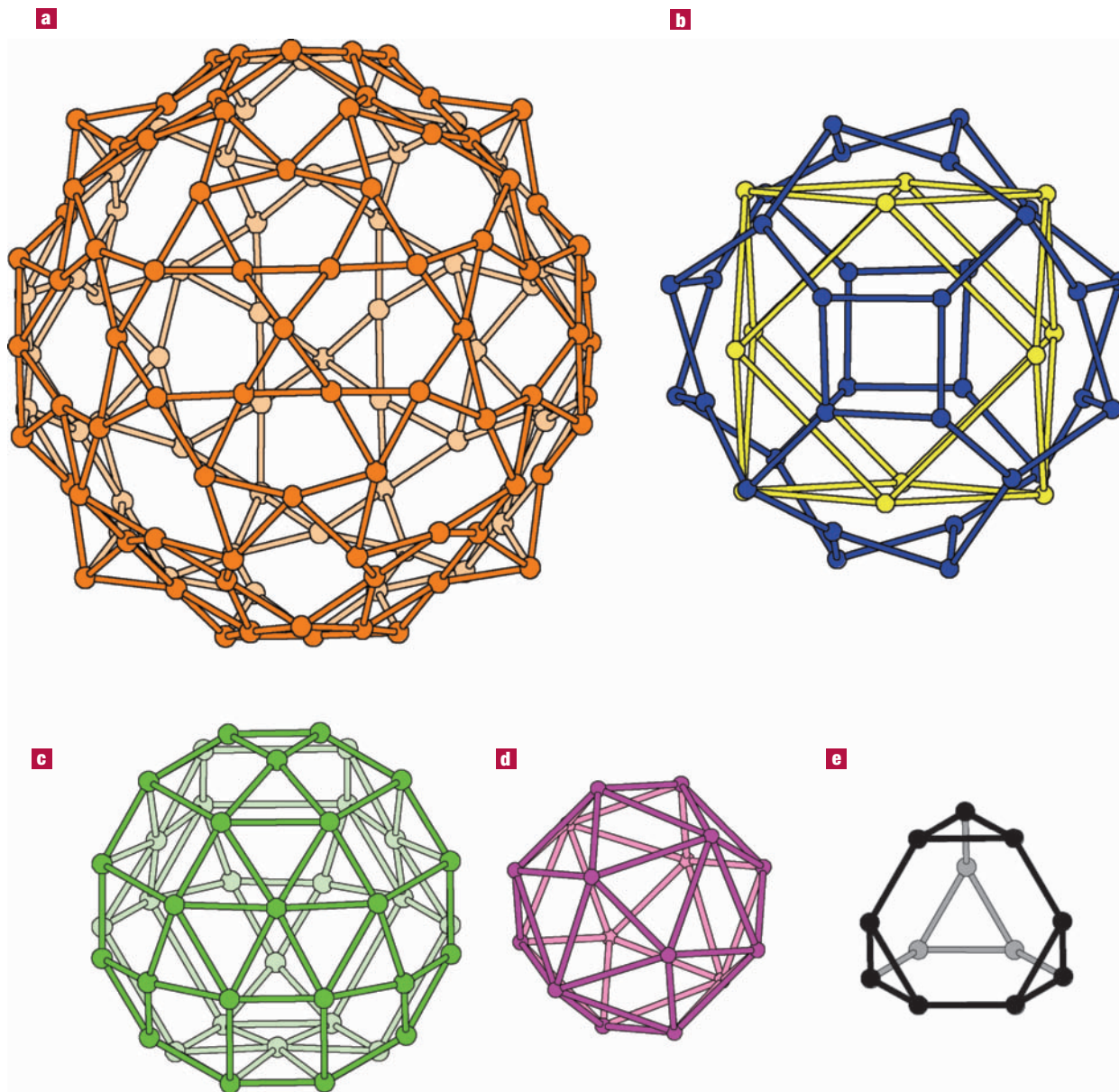
Figure 5 Geometry of the different spheres. **a**, O_{126}; **b**, $Sr_{32}(Bi_{8.25}\square_{3.75})$; **c**, O_{40}; **d**, Bi_{16}; and **e**, O_{12}.

the $6s^2$ lone pair of Bi^{3+} governs the geometry of this pseudo-spherical anion, explaining also the existence of anionic vacancies, leaving room for the extension of its electronic lone pair. It is most probable that this anion, due to its great size and shape, is at the origin of the fullerene-like structure of this aluminate.

In conclusion, a fullerenoid oxide, built up of Al_{84} huge spheres has been synthesized for the first time. The great similarity of this structure to that of the *D2d* isomer of C_{84} fullerenes opens the route to the exploration of other possible members in this series, varying the size of the Al_n spheres, and their mode of connection by changing the nature and the amount of alkaline-earth cations with respect to the tetrahedral aluminium species, but also by considering the possibility of introducing other tetrahedral species on the aluminium sites, such as Si, Ge, Ga, Fe and so on, and other cations or anions inside the Al_n sphere. As a consequence, these materials should rather be regarded as potential

for various properties and applications ranging from photoluminescence or thermoluminescence to magnetism, frequency doubling or nonlinear optical properties, and even to catalysis.

METHODS

The X-ray structure determination of this aluminate was carried out on a crystal of $0.111 \times 0.60 \times 0.05$ mm³. The data were collected with a Brucker–Nonius Kappa CCD four-circle diffractometer equipped with a CCD detector and using the MoKα radiation. The reciprocal space was registered up to $\theta = 30°$, leading to a total of 8,153 reflections and 1,305 independent reflections with $I > 3\sigma (I)$. With 90 refined parameters, the agreement factors are $R(F_o) = 0.0400$ and $R_w(F_o^2) = 0.0818$. F_o and F_c are the observed and calculted structure factors and $R(F_o) = (\Sigma ||F_o| - |F_c||)/(\Sigma |F_o|)$, whereas
$R_w = \{\Sigma [w (F_o^2 - F_c^2)^2]/\Sigma [w(F_o^2)^2]\}^{1/2}$, where $w = 1/[\sigma^2(F_o^2) + (0.0401P)^2]$; $\sigma(F_o^2)$ is the error on F_o^2, and $P = (\max(F_o^2,0) + 2F_c^2)/3$.

The electron-diffraction study was carried out with a JEOL 2010 electron microscope and the high-resolution electron microscopy with a TOPCON 002B (200 kV-Cs = 0.4 mm). Both microscopes
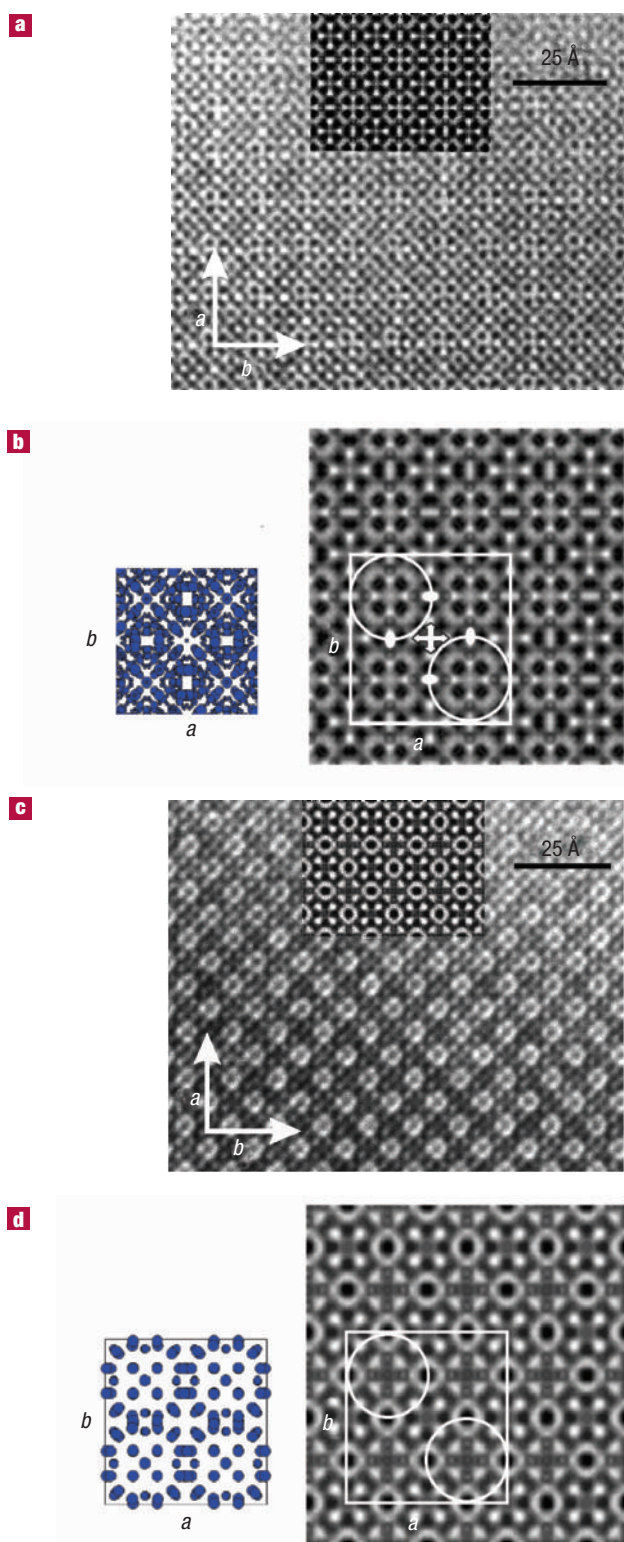
Figure 6 **HREM evidence of the structural specificities of the fullerenoid aluminate.** **a,b**, HREM images of the basal plane (**a**) and projection of the single unit cell (blue coloured) in relation to the enlarged image (**b**) for a focus value close to where the high-electron-density zones appear as dark spots. **c,d**, HREM image (**c**) and projection of the $Sr_{32}(Bi_{8.25}\square_{4.75})$ spheres in relation to the enlarged image (**d**). The white squares represent the unit cell, whereas the circles and elongated white sticks outline the characteristic structural units at the origin of the contrast.
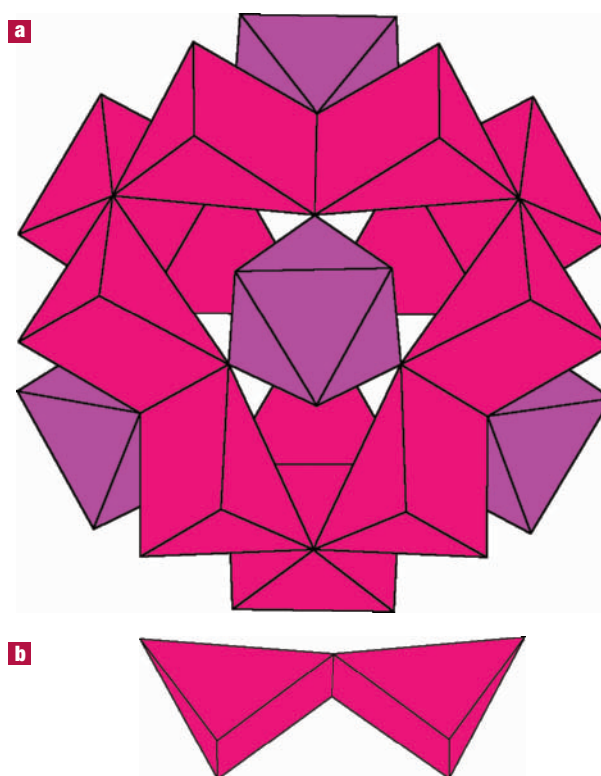
Figure 7 **Pseudo-spheric anion located in the heart of the spheres. a,b**, Geometry of the $Bi_{16}O_{48-n}\square_n$ anion (**a**) forming Bi_2O_8 units of two edge-sharing BiO_5 pyramids (**b**) associated to BiO_6 octahedra.

were equipped with energy-dispersive spectrometers. The image calculations were carried out with MacTempas software.

References

1. Ohta, M., Maruyama, M., Hayakawa, T. & Nishijo, T. Role of dopant on long-lasting phospor of strontium aluminate. *J. Ceram. Soc. Jpn* **108,** 284–289 (2000).
2. Mandelcorn, L. (ed.) *Non-Stoichiometric Compounds* (Academic, New York, 1964).
3. Helfferich, F. *Ion Exchange Properties* (McGraw-Hill, New York, 1962).
4. Wilson, S. T., Lok, B. M., Masina, C. A., Cannan, T. R. & Flanigen, E. H. Aluminophosphate molecular sieves: a new class of microporous crystalline inorganic solids. *J. Amer. Chem. Soc.* **104,** 1146–1147 (1982).
5. Guth, J. L., Kessler, H. & Wey, R. *Stud. Surf. Sci. Catal.* **28,** 121 (1986).
6. Cheetham, A. K., Ferey, G. & Loiseau, T. Open-framework in inorganic materials. *Angew. Chem. Intl Edn* **38,** 3268–3282 (1999).
7. Rabo, J. A. & Schoonover, M. W. Early discoveries in zeolite chemistry and catalysis at Union Carbide and follow up in industrial catalysis. *Appl. Catal. A* **222,** 261–275 (2001).
8. Zones, S. I. & Davis, M. E. Zeolite materials: recent discoveries and future prospects. *Curr. Opin. Solid State Mater. Sci.* **1,** 107–117 (1996).
9. OKeefe, M., Eddaoudi, L. H., Reineke, T. & Yaghi, O. M. Frameworks for extended solids: geometrical design principles. *J. Solid State Chem.* **152,** 3–20 (2000).
10. Férey, G. Building units design and scale chemistry. *J. Solid State Chem.* **152,** 37–48 (2000).
11. Wells, A. F. *Structural Inorganic Chemistry* 5th edn (Oxford Univ. Press, Oxford, 1993).
12. Smith, J. V. Topochemistry of zeolites and related materials 1. Topology and geometry. *Chem. Rev.* **88,** 149–182 (1988).
13. Krätschner, W., Lamb, L. D., Fostiropoulos, K. & Huffman, D. R. Solid C_{60}: a new form of carbon. *Nature* **347,** 354–358 (1990).
14. Okada, S. & Saito, S. Number of extractable fullerene isomers and speciality of C_{84}. *Chem. Phys. Lett.* **252,** 94–100 (1996).
15. Bakakin, V. V. *et al.* The structure of frame strontium aluminate $Sr_6(Al_{12}O_{24})Bi_2O_3$ with inclusion of Bi_2O_3 molecule. *Zh. Strukt. Khim.* **35,** 92–99 (1994).

Correspondence and requests for materials should be addressed to M.H.